Journal of Solid State Chemistry 183 (2010) 93–98

Contents lists available at ScienceDirect

Journal of Solid State Chemistry

journal homepage: www.elsevier.com/locate/jssc

Proton conductivity of potassium doped barium zirconates

Xiaoxiang Xu [a], Shanwen Tao [a,b,*], John T.S. Irvine [a]

[a] School of Chemistry, University of St. Andrews, Fife KY16 9ST, UK
[b] Department of Chemistry, Heriot-Watt University, Edinburgh EH14 4AS, UK

ARTICLE INFO

Article history:
Received 7 May 2009
Received in revised form
19 October 2009
Accepted 25 October 2009
Available online 31 October 2009

Keywords:
$BaZrO_3$
Proton conductivity
Potassium
Impedance measurement
Fuel cell

ABSTRACT

Potassium doped barium zirconates have been synthesized by solid state reactions. It was found that the solubility limit of potassium on *A*-sites is between 5% and 10%. Introducing extra potassium leads to the formation of second phase or YSZ impurities. The water uptake of barium zirconates was increased even with 5% doping of potassium at the *A*-site. The sintering conditions and conductivity can be improved significantly by adding 1 wt% ZnO during material synthesis. The maximum solubility for yttrium at *B*-sites is around 15 at% after introducing 1 wt% zinc. The conductivity of $Ba_{0.95}K_{0.05}Zr_{0.85}Y_{0.11}Zn_{0.04}O_{3-\delta}$ at 600 °C is 2.2×10^{-3} S/cm in wet 5% H_2. The activation energies for bulk and grain boundary are 0.29(2), 0.79(2) eV in wet 5% H_2 and 0.31(1), 0.74(3) eV in dry 5% H_2. A power density of 7.7 mW/cm^2 at 718 °C was observed when a 1 mm thick $Ba_{0.95}K_{0.05}Zr_{0.85}Y_{0.11}Zn_{0.04}O_{3-\delta}$ pellet was used as electrolyte and platinum electrodes.

1. Introduction

Proton conducting ceramics have a wide range of possible applications such as gas sensors, hydrogen pumps and membrane reactors, etc. [1]. Their potential application as electrolytes in fuel cells were considered as a promising way to reduce greenhouse gas emissions [2]. Perovskite oxides based on $SrCeO_3$ have been recognized to exhibit predominant proton conduction under hydrogen containing atmosphere at elevated temperatures many years ago [3]. Thereafter numerous perovskite oxides with similar compositions have been synthesized and investigated such as $CaZrO_3$ [4–6] and $BaCeO_3$ [7–10]. Their chemical compositions could be written as $AB_{1-x}M_xO_{3-\delta}$, where *M* is some trivalent element such as a rare earth and δ is the oxygen deficiency per perovskite unit cell. Among the perovskite oxides investigated, cerate-based oxides generally present the highest conductivity but suffer from decomposition under atmospheres containing CO_2 or H_2O below 500 °C [11,12]. Great efforts have been devoted to partially substitute cerium with zirconium or by the introduction of other elements such as Gd, Nd or Co in the hope to improve the stability [13–16]. It has been found that the stability of these partially replaced cerates depends strongly on the zirconium content [14], in other words, complete replacement of cerium for zirconium is expected to exhibit the highest stability under atmospheres containing CO_2 and H_2O therefore allowing hydrocarbon fuels to be utilized. Although zirconates such as doped $BaZrO_3$ demonstrate similar conducting behavior to cerates in terms of formation and mobility of protonic charge carriers [17], their conductivity is usually one order of magnitude lower than cerates [1]. This is attributed to the highly refractory properties of zirconates with low rates of grain growth under typical sintering conditions which limit the overall proton transport [17]. This explanation has been confirmed by annealing the zirconates at a high temperature (~2200 °C) where the grain boundary conductivity was improved by nearly two orders of magnitude [18]. However, high temperature sintering should be avoided due to loss of barium at high temperature which is one factor that leads to a diminished conductivity [19]. Besides, from a technological point of view, high sintering temperatures introduce difficulties and unfavorable cost in manufacturing the materials since other auxiliary materials such as electrodes in fuel cells can hardly sustain such a high temperatures, never mind the likelihood of interfacial reaction [20]. Introducing zinc oxide into the *B*-sites is an efficient way in improving sintering conditions while conductivity is still unsatisfactory compared with cerates. On the other hand, proton conductivity of perovskite oxides was found to be strongly affected by the basicity of the constituent oxides due to its dominant influence on water uptake capacity [21], introducing highly basic alkaline oxides should improve the conductivity. Alkaline ions are more preferable to be doped at *A*-sites where crystal structure could be maintained. Patnaik et al. [22] did some fundamental work on *A*-site potassium doped barium zirconates, they found that the *A*-site potassium doped barium zirconates showed a significantly higher conductivity than *A*-site undoped barium zirconates where the yttrium dopant

* Corresponding author at: Department of Chemistry, Heriot-Watt University, Edinburgh EH14 4AS, UK.
E-mail address: s.tao@hw.ac.uk (S. Tao).

0022-4596/$ - see front matter © 2009 Elsevier Inc. All rights reserved.
doi:10.1016/j.jssc.2009.10.017

contents on *B*-site are approximately equal. However, some impurities (ZrO_2) remained in their samples and pure *A*-site potassium doped barium zirconates were not synthesized successfully in their work. One possible reason is that the limit for potassium doping at *A*-site is lower than 10%. In this paper, samples in series $Ba_{1-x}K_xZr_{1-y}Y_yO_{3-\delta}$ ($x \le 0.15$, $y \le 0.2$) with and without zinc doping have been synthesized. The conductivity of the samples in different atmospheres has also been investigated.

2. Experimental

2.1. Material synthesis

All samples were synthesized by conventional solid state reaction methods. Calculated amounts of $BaCO_3$, ZrO_2, Y_2O_3, K_2CO_3, ZnO were mixed according to the desired compositions. The oxides were preheated at 500 °C prior to weighing in order to remove the adsorbed water and gases. The mixtures were then planetary ball milled in a zirconia container with zirconia balls in the presence of acetone to ensure thorough mixing. The finely ground materials were fired at 1400 °C for 10 h with intermediate grindings. For samples without zinc, the fired powders were subsequently ground using a mortar and pestle before pressing into pellets under a pressure of 500 MPa. The pellets were fired at 1450 °C again for another 10 h before conductivity measurements. For samples with zinc, the precursors (apart from zinc) according to the formula were mixed and pre-fired at 1100 °C to decompose the carbonates then a calculated amount of zinc oxide was mixed together with as-fired powders, ball-milled for 30 min and pressed into pellets in a diameter of 13 mm before firing at 1300 °C for 10 h.

2.2. Materials characterization and conductivity measurements

Crystal structure and phase purity were examined by X-ray diffraction (XRD) analysis of powders on a Stoe STADI/P powder diffractometer. Incident radiation was generated using a Cu*K*α1 source (λ=1.54056 Å). The step size for data collection was 0.02° with a collection time 10 s at each step. Vaseline was used to mount the sample in the holder. X-POW software was used to perform least square refinement of the lattice parameters of the samples. Thermal analysis was carried out on a Rheometric Scientific TG 1000M+ and TA instruments with heating and cooling rate of 5 °C/min under flowing dry Ar, dry and wet 5% H_2/Ar (humidified in water at 20 °C) at a rate of 20 mL/min. The microstructure of pellets was inspected by scanning electron microscope (SEM) on a JEOL 5600 SEM with a Mica energy dispersive X-ray spectroscopy (EDS) analysis system. EDS on cross-section of a $Ba_{0.95}K_{0.05}Zr_{0.85}Y_{0.11}Zn_{0.04}O_{3-\delta}$ pellet was carried out at a voltage of 20 kV and spot size of 45. Sample for EDS analysis was prepared by mechanical breaking without further treatment. An Agilent 7500a inductively coupled plasma mass spectroscopy (ICP-MS) with laser ablation was used for surface element analysis.

Conductivity was investigated by a.c. impedance method over the frequency range from 1 MHz to 0.1 Hz at 100 mV r.m.s. using a Schlumberger Solartron 1255 Frequency Response Analyzer coupled with a 1287 Electrochemical Interface controlled by Zplot electrochemical impedance software. Pellets obtained above were coated with conductive platinum paste on both sides serving as electrodes and were then fired at 900 °C to ensure good ohmic contact. Measurements were performed from 200 to 850 °C on cooling under ambient air, wet 5% H_2/Ar (humidified at 20 °C in water), dry 5% H_2/Ar (desiccated at 20 °C in 98% H_2SO_4). Accordingly, the steam vapor pressures are 8.4×10^{-4}, 3.0×10^{-2} and 1.3×10^{-6} atm for air, wet and dry 5% H_2, respectively [23]. Pellets were maintained at 850 °C for at least 12 h in each atmosphere and impedance data were collected at 50 °C steps after 1 h dwell at each step for equilibrium.

3. Results and discussions

3.1. Phase composition

X-ray powder diffraction was carried out on each of prepared samples; XRD patterns for samples without zinc are shown in Fig. 1. Single phase perovskite oxides were formed on doping 5% potassium onto the *A*-site and 10% yttrium onto *B*-site; a second perovskite-like phase and YSZ (yttrium stabilized zirconium) appeared when 10% or more potassium was introduced, implying the upper limit of solid solution formation on *A*-sites for potassium is between 5% and 10%. This could be a reason why Patnaik et al. did not obtain a pure potassium doped $BaZrO_3$, where more than 10% potassium was used [22]. The unit cell parameter of $Ba_{0.95}K_{0.05}Zr_{0.9}Y_{0.1}O_{3-\delta}$ (4.2075(6) Å) is close to the reported value for $BaZr_{0.9}Y_{0.1}O_{3-\delta}$ [24] (4.2044 Å) which is plausible due to the similar average ionic radius of Ba^{2+} (1.60 Å) and K^+ (1.60 Å) at 12 coordinates [25]. However, the experimental density of $Ba_{0.95}K_{0.05}Zr_{0.9}Y_{0.1}O_{3-\delta}$ pellets fired at 1450 °C only reached 60% of its theoretical density (calculated using lattice parameters from XRD data) due to the refractory properties of barium zirconates. Dense pellets were not obtained even when the sintering temperature was increased to 1600 °C indicating that potassium oxide is not an efficient sintering aid for barium zirconates.

3.2. Thermogravimetric and water uptake studies

Thermogravimetric studies were carried out by recording the weight change against temperature in different atmospheres (dry and wet 5% H_2 (humidified at 20 °C)). Samples for TG studies were pre-treated in dry Ar at 900 °C for 5 h to eliminate water and the temperature was controlled from 900 to 20 °C at a cooling rate of 5 °C/min. Fig. 2 shows the weight changes in different atmospheres. In dry 5% H_2, the as-prepared sample shows a weight change $<0.25\%$ from 900 to 20 °C. This weight change can

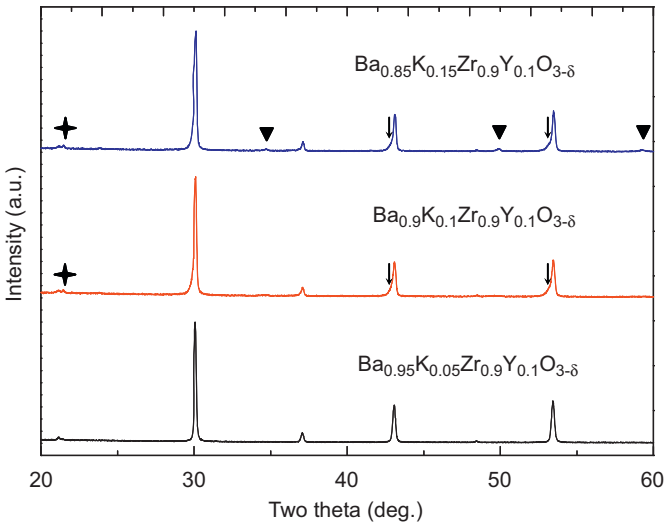

Fig. 1. X-ray diffraction patterns of samples prepared: ✦, vaseline peak; ▼, YSZ peaks; ↓, second phase.

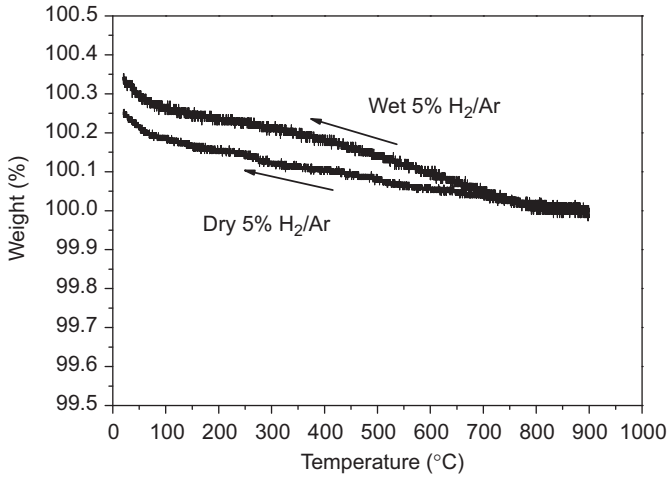

Fig. 2. TGA patterns of $Ba_{0.95}K_{0.05}Zr_{0.9}Y_{0.1}O_{3-\delta}$ in dry and wet 5% H_2, the samples were pre-treated in dry Ar at 900 °C for 5 h. The flow rate of gas was controlled at 20 ml/min and the cooling rate is 5 °C/min.

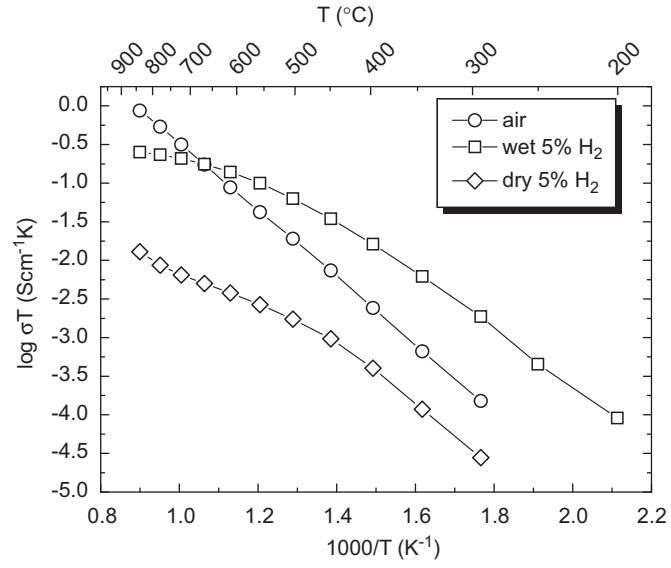

Fig. 3. Conductivity of $Ba_{0.95}K_{0.05}Zr_{0.9}Y_{0.1}O_{3-\delta}$ in differently atmospheres.

arise from the buoyancy since density of the gas is changed with temperature. On the contrary, almost 0.35% weight increase was observed in wet 5% H_2. The additional 0.1% weight change could be attributed to the absorption of water molecules when samples were exposed to moisture. This is nearly 0.02 water molecules per formula unit correspondingly. Compared with $BaZr_{0.9}Y_{0.1}O_{3-\delta}$ where no significant water change was observed [24], introducing potassium even 5% is an effective way to improve the water uptake.

3.3. Conductivity

The conductivities of as-prepared samples under various atmospheres are shown in Fig. 3. The values were calculated from the Cole–Cole plots obtained by a.c. impedance spectra (not shown). For the conductivity in air, a linear relationship versus reciprocal temperature was observed indicating a single activation process. The activation energy is 0.86 eV calculated from the slope. According to Iwahara et al. [1], these perovskite-type ceramics exhibit p-type electronic (hole) conduction under oxidizing atmospheres by the following equation:

$$O_2 + 2V_O^{\bullet\bullet} \leftrightarrow 4h^{\bullet} + 2O_O^{\times} \quad (1)$$

However, in a wet reducing atmosphere, the Arrhenius plots of conductivity shows a different linear trend with large deviations at high temperatures. The activation energy from 300 to 600 °C is 0.61 eV. The ceramics were deemed to become a proton conductor in the presence of water vapor and hydrogen by equation:

$$H_2O(g) + O_O^{\times} + V_O^{\bullet\bullet} \leftrightarrow 2(OH)_O^{\bullet} \quad (2)$$

However, in dry 5% H_2 (steam vapor pressure 1.3×10^{-6} atm), the conductivity was significantly lower than that in air and wet 5% H_2. It was found that the conductivity of the potassium doped samples in wet reduced atmospheres at 600 °C was improved substantially (from 5.78×10^{-5} [24] to 1.5×10^{-4} S/cm compared to the potassium-free sample); however, the conductivity is still lower than similar compounds containing cerium [26].

3.4. Addition of ZnO at B-sites while fixing A-site at 5 mol% K

The poor conductivity of $Ba_{0.95}K_{0.05}Zr_{0.9}Y_{0.1}O_{3-\delta}$ was probably due to the low density causing grain boundary resistance to dominate the conduction process and the low defect concentration that only 10% of zirconium was replaced by yttrium. To improve the sinterability and conductivity, zinc oxide and additional yttrium were introduced. In our previous work, it was found that barium zirconates can be well sintered at 1325 °C by introducing 1 wt% ZnO which is 4% mol ratio at the *B*-site [26]. In this experiment, ZnO content was fixed at 4 mol% and yttrium content was varied. Fig. 4 shows the XRD patterns for $Ba_{0.95}K_{0.05}Zr_{0.8}Y_{0.16}Zn_{0.04}O_{3-\delta}$ and $Ba_{0.95}K_{0.05}Zr_{0.85}Y_{0.11}Zn_{0.04}O_{3-\delta}$. It was found that introducing 5% more yttrium leads to the separation of Y_2O_3 (or yttrium stabilized zirconia) from the perovskite structure therefore the up limit of yttrium solid solution in *B*-site lies between 11% and 16% after introducing 4 mol% Zn at *B*-site. The unit cell parameter for $Ba_{0.95}K_{0.05}Zr_{0.85}Y_{0.11}Zn_{0.04}O_{3-\delta}$ is 4.2114(5) Å which is slightly less than for $Ba_{0.97}Zr_{0.8}Y_{0.16}Zn_{0.04}O_{3-\delta}$ (4.2220(4) Å) [20]. The density of $Ba_{0.95}K_{0.05}Zr_{0.85}Y_{0.11}Zn_{0.04}O_{3-\delta}$ reaches 92% of its theoretical density confirming the improved sintering conditions after zinc doping.

Fig. 5 shows the SEM pictures of a $Ba_{0.95}K_{0.05}Zr_{0.85}Y_{0.11}Zn_{0.04}O_{3-\delta}$ pellet fired at 1300 °C for 10 h. Some small pinholes

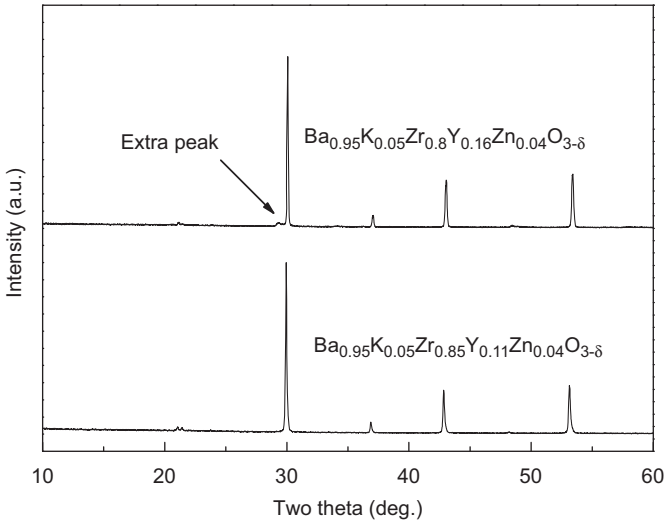

Fig. 4. X-ray diffraction patterns of samples with zinc added. The powders were fired at 1300 °C for 10 h after ZnO was added.

can still be observed between the closely packed grains since the experimental density only reached 92% of the theoretical one. ICP-MS and EDS were used to determine the potassium distribution. Although ICP-MS indicated a deficiency of potassium at the pellet surface, EDS analysis of cross-section in SEM showed a uniform distribution of all elements, including potassium across the entire 2 mm cross-section of the pellet (Fig. 6). The content of potassium and zinc was estimated 2.8 ± 1.7 and 2.5 ± 1.4 mol%, respectively, indicating the presence of both elements. From the EDS profile, the depth resolution was estimated as $<5\,\mu m$ hence the material was essentially homogeneous. Due to the relative large spot size, it is difficult to decide whether potassium is at the grain or grain boundary through only SEM-EDS analysis.

Typical impedance spectra of $Ba_{0.95}K_{0.05}Zr_{0.85}Y_{0.11}Zn_{0.04}O_{3-\delta}$ at low temperatures (200 °C) in dry and wet 5% H_2/Ar are shown in Fig. 7. All impedance data can be well fitted using equivalent circuit present (Fig. 7). Throughout the entire frequency range, only two depressed semicircles can be separated. The first high frequency semicircle (geometrical capacitance $\sim 3 \times 10^{-9}$ F/cm) could be assigned to the grain boundary response and the second low frequency semicircle (geometrical capacitance $\sim 1 \times 10^{-6}$ F/cm) is a typical response for a electrode process [27]. The bulk response, however, could not be clearly separated from the impedance spectra through the whole temperature range (200–800 °C), probably the bulk response is masked by that from grain boundary. It is clear that $Ba_{0.95}K_{0.05}Zr_{0.85}Y_{0.11}Zn_{0.04}O_{3-\delta}$ exhibits lower grain boundary and total resistances in the wet 5% H_2 than in dry 5% H_2 indicating proton conduction.

Fig. 8 shows the Arrhenius plot of total conductivity for $Ba_{0.95}K_{0.05}Zr_{0.85}Y_{0.11}Zn_{0.04}O_{3-\delta}$ as a function of temperature in different atmospheres. The values were calculated from fitting of the impedance spectra using the equivalent circuit shown (Fig. 7). The total conductivity, in all three atmospheres, was improved significantly (more than one magnitude) as compared with samples without zinc. The effect of doping potassium at *A*-site can be evaluated by comparing zinc-containing samples with and without potassium. A typical total conductivity in wet 5% H_2 for $Ba_{0.95}K_{0.05}Zr_{0.85}Y_{0.11}Zn_{0.04}O_{3-\delta}$ is 2.2×10^{-3} S/cm at 600 °C which is two times higher than $Ba_{0.97}Zr_{0.8}Y_{0.16}Zn_{0.04}O_{3-\delta}$ (1×10^{-3} S/cm) reported [20]. The conductivity reached a plateau at a temperature above 450 °C in 5% H_2 which is a typical behavior for these types of proton-conducting perovskite oxides [20,24]. The grain boundary and bulk conductivity (calculated by subtracting grain boundary resistance from total resistance) below 400 °C in wet and dry 5% H_2 were plotted together with total conductivity for comparison (Fig. 9). It can be seen that bulk conductivity is significantly higher than that for grain boundary at lower temperature and the total conductivity was dominated by grain boundary at low temperatures. The activation energy between 100 and 300 °C calculated from the slope is listed in Table 1. The

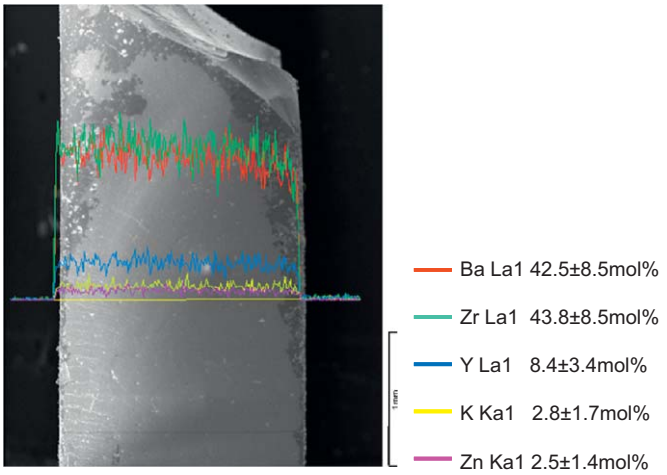

Fig. 6. EDS linear scanning of $Ba_{0.95}K_{0.05}Zr_{0.85}Y_{0.11}Zn_{0.04}O_{3-\delta}$ pellet cross-section. The element content was estimated according to the area of each spectrum (scanning time was 30 min).

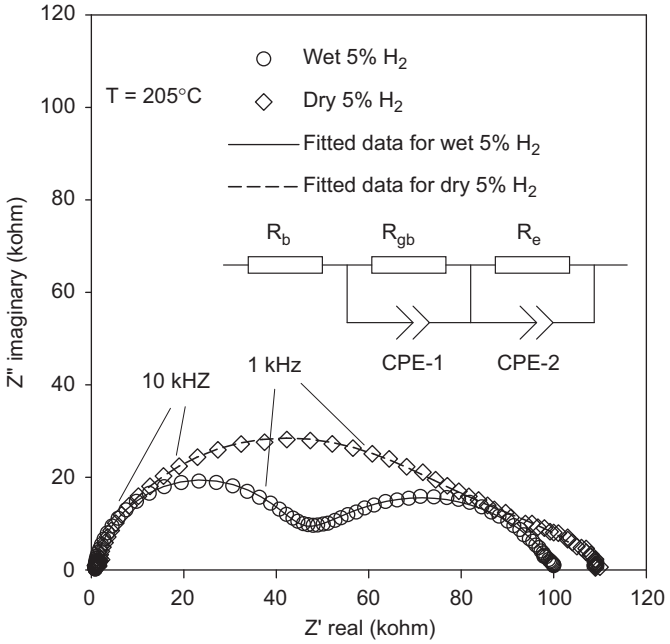

Fig. 7. Complex impedance diagrams for $Ba_{0.95}K_{0.05}Zr_{0.85}Y_{0.11}Zn_{0.04}O_{3-\delta}$ at 205 °C in dry and wet 5% H_2. Equivalent circuit that used to calculate the resistance was inserted in the diagrams.

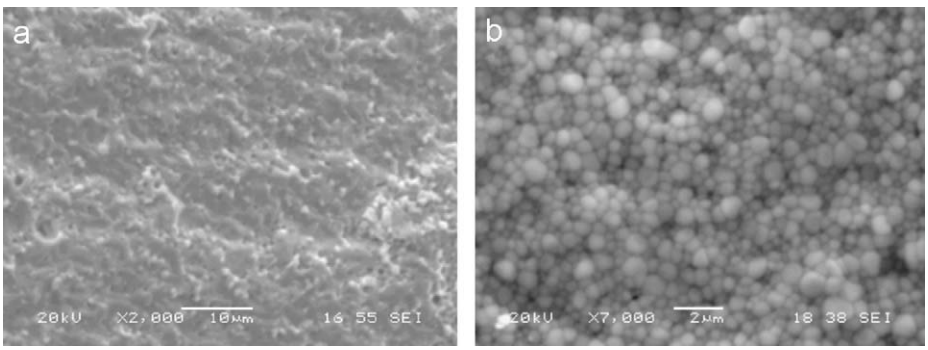

Fig. 5. SEM picture of $Ba_{0.95}K_{0.05}Zr_{0.85}Y_{0.11}Zn_{0.04}O_{3-\delta}$ pellet fired at 1300 °C for 10 h: cross-section (a) and surface (b).

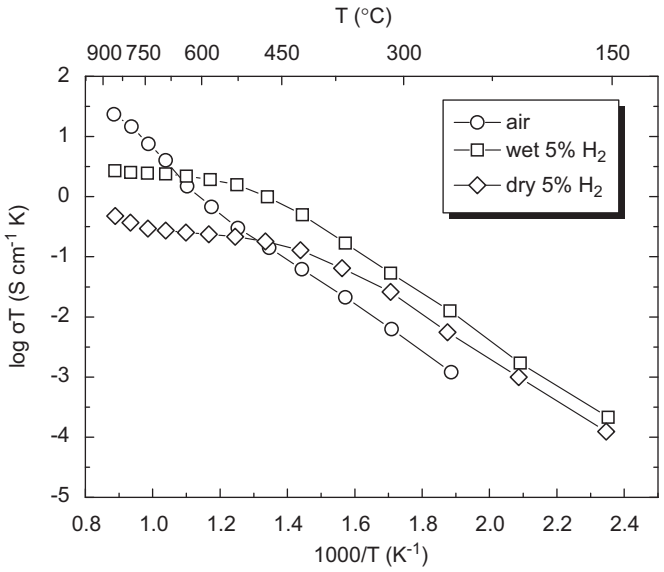

Fig. 8. Conductivity of $Ba_{0.95}K_{0.05}Zr_{0.85}Y_{0.11}Zn_{0.04}O_{3-\delta}$ in different atmospheres.

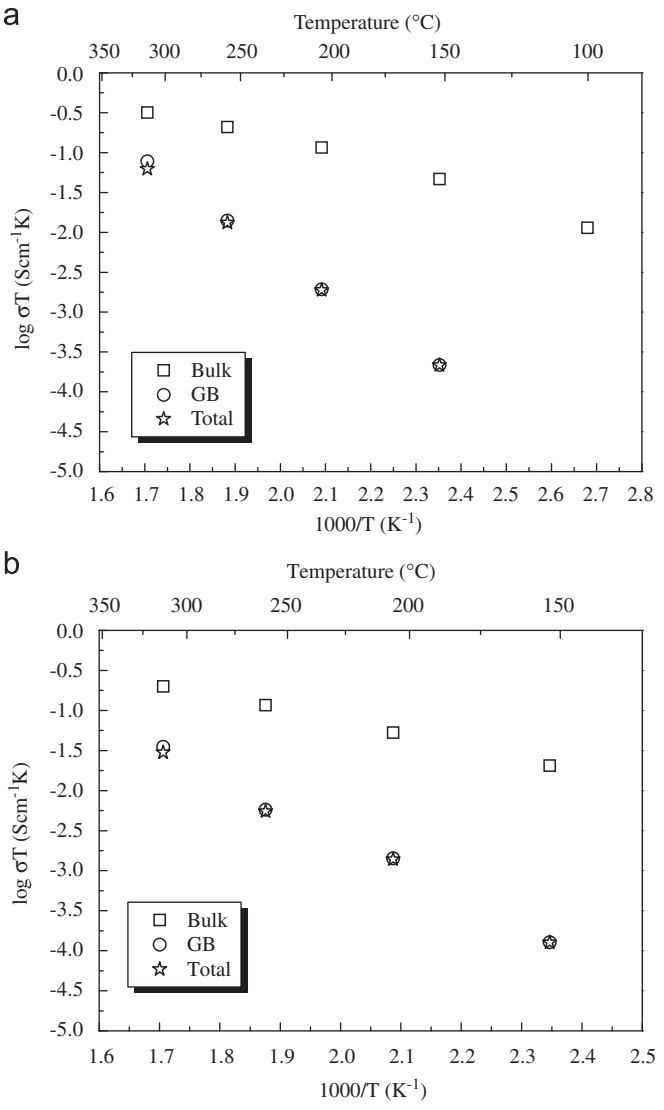

Fig. 9. Bulk, grain boundary and total conductivity of $Ba_{0.95}K_{0.05}Zr_{0.85}Y_{0.11}Zn_{0.04}O_{3-\delta}$ between 100 and 300 °C in wet (a) and dry (b) 5% H_2.

Table 1
Activation energy of $Ba_{0.95}K_{0.05}Zr_{0.85}Y_{0.11}Zn_{0.04}O_{3-\delta}$ between 100 and 300 °C in different atmospheres.

	Bulk	Grain boundary	Total
Wet 5% H_2	0.29(2) eV	0.79(2) eV	0.76(1) eV
Dry 5% H_2	0.31(1) eV	0.74(3) eV	0.72(4) eV

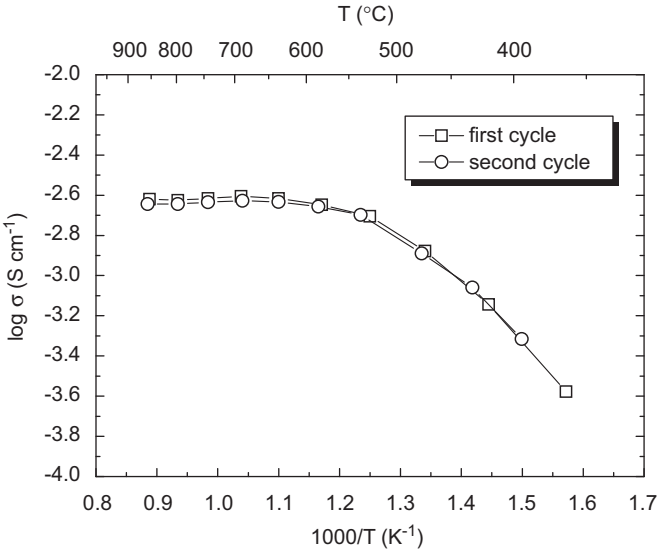

Fig. 10. Conductivity of $Ba_{0.95}K_{0.05}Zr_{0.85}Y_{0.11}Zn_{0.04}O_{3-\delta}$ in wet 5% H_2 for two cycles.

obtained values for bulk in wet and dry 5% H_2 are 0.29(2) and 0.31(1) eV while for grain boundary; the activation energy are 0.79(2) and 0.74(3) eV respectively. It should be noted that the activation energy for bulk conduction is significantly lower than the reported values. One possible explanation could be the *A*-site doping which may alleviate the proton-dopant trapping effect. Further investigation is required.

The stability of conductivity in wet 5% H_2 was investigated by measuring the conductivity in two cycles both from highest (850 °C) to lowest (200 °C). Fig. 10 shows the results. There is no significant difference between these two cycles suggesting good reproduction of conductivity.

The fuel cell performance based on $Ba_{0.97}Zr_{0.8}Y_{0.16}Zn_{0.04}O_{3-\delta}$ electrolyte has been estimated. Pellets that used as electrolyte were sintered at 1400 °C for 10 h. The thickness of the electrolyte is 1 mm and platinum paste was used as electrodes with effective area 0.2 cm^2. Wet 5% H_2 and air were used as fuels and oxidant respectively. Fig. 11 shows the fuel cell ($Pt/Ba_{0.95}K_{0.05}Zr_{0.85}Y_{0.11}Zn_{0.04}O_{3-\delta}/Pt$) performance in different temperatures. The OCV (open circuit voltage) is 0.81, 0.85 and 0.88 V at 718, 653 and 586 °C, respectively. The OCV is lower than the theoretical values and is decreased with increasing temperature. This seems likely to be due to the contribution of p-type electronic conduction on the air side after doping with potassium [22]. The fuel cell gives a maximum power density 7.7 mW/cm^2 at 718 °C and an overall resistance 4 $\Omega\,cm^2$ (Fig. 12). The calculated conductivity of $Ba_{0.95}K_{0.05}Zr_{0.85}Y_{0.11}Zn_{0.04}O_{3-\delta}$ in the fuel cell, according to a.c. impedance and omitting any correction for electrodes is 0.006, 0.005 and 0.003 S/cm for 718, 653 and 586 °C, respectively. The conductivity for the electrolyte measured separately, however, is about 30% lower, probably implying extension of electrode activity beyond the small Pt-painted region in the fuel cell.

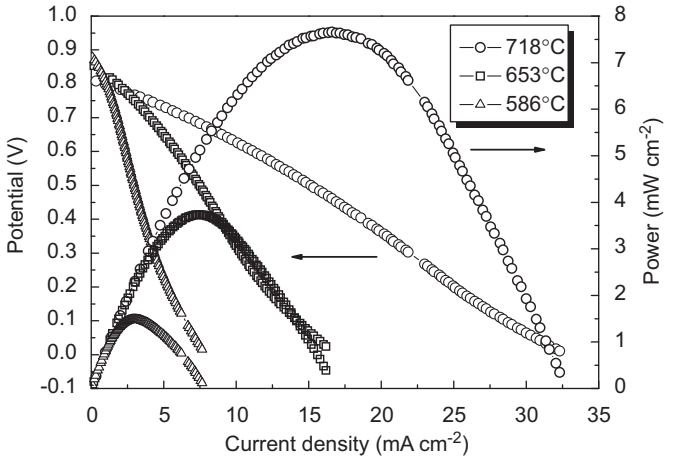

Fig. 11. Fuel cell performance for Pt/ $Ba_{0.95}K_{0.05}Zr_{0.85}Y_{0.11}Zn_{0.04}O_{3-\delta}$/Pt under humidified 5% H_2/air conditions at different temperatures.

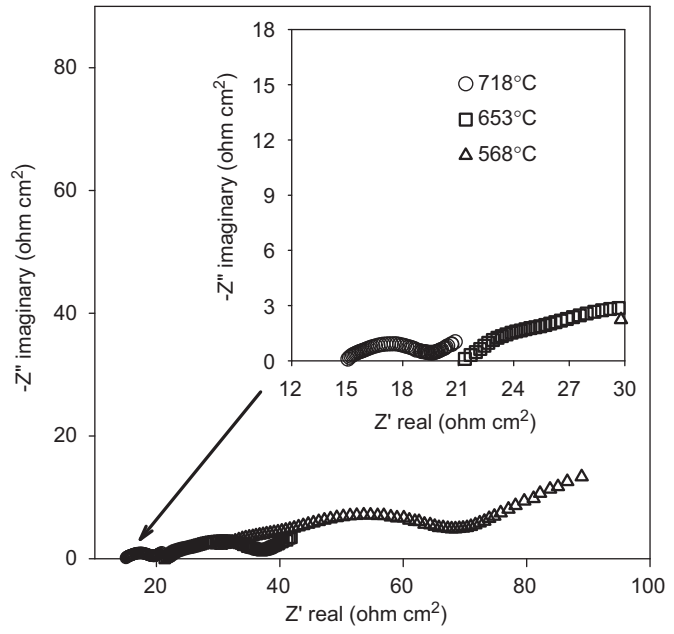

Fig. 12. Complex impedance diagrams under open circuit conditions at different temperatures.

4. Conclusions

Potassium doped barium zirconates were synthesized with different compositions by solid state reaction. The upper limit of solid solution formation on the *A*-sites for potassium is between 5% and 10%. Introducing extra potassium leads to the formation of second phase or YSZ impurities. The water uptake of barium zirconates ($Ba_{0.95}K_{0.05}Zr_{0.9}Y_{0.1}O_{3-\delta}$) was improved even with 5% doping of potassium. The sintering conditions and conductivity can be improved significantly by adding 1 wt% ZnO during material synthesis. The upper limit of solid solution formation in *B*-sites for Yttrium is between 11% and 16% after introducing 1 wt% zinc. The conductivity of $Ba_{0.95}K_{0.05}Zr_{0.85}Y_{0.11}Zn_{0.04}O_{3-\delta}$ at 600 °C is 2.2×10^{-3} S/cm in wet 5% H_2. Fuel cell using $Ba_{0.95}K_{0.05}Zr_{0.85}Y_{0.11}Zn_{0.04}O_{3-\delta}$ pellet (1 mm thick) as electrolyte reached a maximum power density of 7.7 mW/cm^2 when platinum was used as cathode and anode.

Acknowledgments

We thank EPSRC and EaStCHEM for funding. The authors sincerely thank EaStCHEM for a fellowship (Tao) and a studentship (Xu). Irvine thanks EPSRC for a senior Fellowship. Thank Mrs Sylvia Williamson and Dr Cristian Savaniu for help with ICP-MS tests.

References

[1] H. Iwahara, Y. Asakura, K. Katahira, M. Tanaka, Solid State Ionics 168 (2004) 299.
[2] M. Maffei, L. Pelletier, J.P. Charland, A. McFarlan, Fuel cells 4 (2007) 323.
[3] H. Iwahara, T. Esaka, H. Uchida, N. Maeda, Solid State Ionics 3/4 (1981) 359.
[4] T. Higuchi, S. Yamaguchi, K. Kobayashi, S. Shin, T. Tsukamoto, Solid State Ionics 162–163 (2003) 121.
[5] S. Yamaguchi, K. Kobayashi, T. Higuchi, S. Shin, Y. Iguchi, Solid State Ionics 136–137 (2000) 305.
[6] K. Kabayashi, S. Yamaguchi, Y. Iguchi, Solid State Ionics 108 (1998) 355.
[7] S. Yamaguchi, N. Yamada, Solid State Ionics 162–163 (2003) 23.
[8] M. Oishi, K. Yashiro, K. Sato, J. Mizusaki, N. Kitamura, K. Amezawa, T. Kawada, Y. Uchimoto, Solid State Ionics 179 (2008) 529.
[9] S. Yamaguchi, K. Nakamura, T. Higuchi, S. Shin, Y. Iguchi, Solid State Ionics 136–137 (2000) 191.
[10] N. Zakowsky, S. Williamson, J.T.S. Irvine, Solid State Ionics 176 (2005) 3019.
[11] S.V. Bhide, A.V. Virkar, J. Electrochem. Soc. 146 (1999) 4386.
[12] S.V. Bhide, A.V. Virkar, J. Electrochem. Soc. 146 (1999) 2038.
[13] K.H. Ryu, S.M. Haile, Solid State Ionics 125 (1999) 355.
[14] K. Katahira, Y. Kohchi, T. Shimura, H. Iwahara, Solid State Ionics 138 (2000) 91.
[15] C.D. Zuo, S.W. Zha, M.L. Liu, M. Hatano, M. Uchiyama, Adv. Mater. 18 (2006) 3318.
[16] M.A. Azimova, S. McIntosh, Solid State Ionics 180 (2009) 160.
[17] K.D. Kreuer, St. Adams, W. Munch, A. Fuchs, U. Klock, J. Maier, Solid State Ionics 145 (2001) 295.
[18] S.B.C. Duval, P. Holtappels, U.F. Vogt, E. Pomjakushina, K. Conder, U. Stimming, T. Graule, Solid State Ionics 178 (2007) 1437.
[19] P. Babilo, T. Uda, S.M. Haile, J. Mater. Res. 22 (2007) 1322.
[20] S.W. Tao, J.T.S. Irvine, J. Solid State Chem. 180 (2007) 3493.
[21] K.D. Kreuer, Solid State Ionics 97 (1997) 1.
[22] A.S. Patnaik, A.V. Virkar, J. Electrochem. Soc. 154 (2006) A1397.
[23] D.R. Lide, Handbook of Chemistry and Physics, 76th ed, CRC Press, Boca Raton, 1995–1996.
[24] C.D. Savaniu, J. Canales-Vazquez, J.T.S. Irvine, J. Mater. Chem. 15 (2005) 598.
[25] R.D. Shannon, C.T. Prewitt, Acta Crystallogr. B 25 (1969) 925.
[26] S.W. Tao, J.T.S. Irvine, Adv. Mater. 18 (2006) 1581.
[27] J.T.S. Irvine, D.S. Sinclair, A.R. West, Adv. Mater. 2 (1990) 132.